KSTLE International Journal, Vol. 1, No. 2, December 2000, pp. 76-82

Study on Flow Mixing Effects in a High-Speed Journal Bearing

Sang Myung Chun†

Graduate School of Automotive Engineering, Kookmin University, Korea

Abstracts : Turbulence in journal bearing operation is examined and the thermal variability is studied for isothermal, convective and adiabatic conditions on the walls under aligned and misaligned conditions. Also, the effects of a contraction ratio at the cavitation region and the mixing between re-circulating oil and inlet oil on the fluid field of oil film are included. An algorithm for the solution of the coupled turbulent Reynolds and energy equations is used to examine the effects of the various factors. Heat convection is found to play only a small role in determining friction and load under no mixing condition. However, under realistic mixing condition, the heat convection cannot be ignored. The wall temperature and heat transfer have been found to be of secondary important factors to the mixing effectiveness at the groove and the final mixture temperature.

Key words : flow mixing, contraction ratio, turbulence, high-speed journal bearing, shaft misalignment

Introduction

Turbulent motion results in significant increase in friction and changes to pressure and temperature and is induced when the local Reynolds number exceeds a certain critical value. It usually occurs at high surface speeds when the Reynolds number, based on h, exceeds 2000 approximately, that may result in flow instability and hence turbulence. Such high-speed applications include turbocharger bearings of internal combustion engines. However, under certain special conditions associated with bearings of large dimensions (large clearances) or a fluid with a low kinematic viscosity used as a lubricant, turbulence may also occur at the lower velocities.

The onset of turbulence in connection with rotating bearings did not become evident until Wilcock [1] discovered its effects on bearing performance by series of experiments. The basic turbulent lubrication theory has been developed by several researchers [2-7]. And Hashimoto [8] extended the analysis with surface roughness effects. Others [9-13] dealt with practical problems analytically and numerically. Suganami and Szeri [9] showed that an insulated shaft assumption leads to results closer to experimental values. In this paper, the effects of thermal variability including isothermal, convective and adiabatic conditions on the walls under aligned and misaligned conditions are numerically investigated. In addition, a contraction ratio at the cavitation region and the mixing between re-circulating oil and inlet oil are included. Also, in order to examine speed effects on journal bearing, the friction distribution in three-dimensions comparing with the results of laminar flow is investigated.

†Corresponding author; Tel: 82-2-910-4806, Fax: 82-2-910-4718
E-mail: smchun@kmu.kookmin.ac.kr

Governing Equations

For turbulent flow conditions, each parameter is represented by a time-averaged value with Reynolds decomposition, i.e. instantaneous values are the sum of the time-averaged mean values and the deviation from it [14]. Here, for a liquid lubricant, the density is assumed to be constant.

The Reynolds equation [2,3] for a steadily loaded journal bearing for finite width may be written as

$$\frac{\partial}{\partial x}\left(\frac{\rho h^3}{\mu}G_x\frac{\partial \bar{p}}{\partial x}\right)+\frac{\partial}{\partial z}\left(\frac{\rho h^3}{\mu}G_x\frac{\partial \bar{p}}{\partial z}\right)=\frac{U}{2}\frac{\partial(\rho h)}{\partial x}. \tag{1}$$

The appropriate values of G_x and G_z are given by the following [4,5] in the range $1{,}000 \le Re \le 30{,}000$.

$$G_x = \frac{1}{12+0.0136\left(\frac{\rho hU}{\mu}\right)^{0.9}}. \tag{2}$$

$$G_z = \frac{1}{12+0.0043\left(\frac{\rho hU}{\mu}\right)^{0.96}}. \tag{3}$$

For the steady state, two dimensional, incompressible flow of a Newtonian fluid, an energy equation [5-7] with heat transfer boundary conditions at the bearing walls may be derived under turbulence conditions as

$$\rho\left\{\left(\frac{Uh}{2}-\frac{h^3}{\mu}G_x\frac{\partial \bar{p}}{\partial x}\right)\frac{\partial(C_p\bar{T})}{\partial x}-\frac{h^3}{\mu}G_z\frac{\partial \bar{p}}{\partial z}\frac{\partial(C_p\bar{T})}{\partial z}\right\}=$$
$$\tau_c U+\frac{h^3}{\mu}\left\{G_x\left(\frac{\partial \bar{p}}{\partial x}\right)^2+G_z\left(\frac{\partial \bar{p}}{\partial z}\right)^2\right\}-(q_{sT}+q_{bT}) \tag{4}$$

where

$$q_{sT} = H_s(\bar{T} - T_s)$$

and

$$q_{bT} = H_b(\bar{T} - T_b).$$

The values of H_s and H_b [15] are chosen as shown in Table 1. Here, for a liquid lubricant, the specific heat can be assumed to be constant.

In the range 1,000≤Re≤30,000, appropriate values of $\bar{\tau}_c (=\tau_c/\frac{\mu U}{h})$ are given by the following [4,5]:

$$\bar{\tau}_c = 1 + 0.0012\left(\frac{\rho U h}{\mu}\right)^{0.94}. \quad (5)$$

The viscosity is considered to vary with temperature exponentially according to the usual, simplified form:

$$\mu = \mu_o exp\{-\alpha(\bar{T} - T_{in})\}. \quad (6)$$

Film thickness, h, can be defined by the expression:

$$h = c\{1 + \varepsilon cos(\theta - \varphi)\}. \quad (7)$$

where $\varepsilon(z) = \sqrt{\{\varepsilon^2{}_o + 2\eta\varepsilon_o cos(\phi - \varphi_o) + \eta^2\}}$,

$\varphi(z) = \varphi_o + arctan\left(\frac{\eta sin(\phi - \varphi_o)/\varepsilon_o}{1 + \eta cos(\phi - \varphi_o)/\varepsilon_o}\right)$ and

$\eta = \beta z/c$.

The degree of misalignment, D_m [16], is defined as

$$D_m = \eta_e/\eta_m, \quad (8)$$

where η_e is misalignment ratio at both bearing ends, and η_m is the maximum possible value of η_e.

Boundary Conditions

The pressure at the ends of a finite length bearing is taken to be equal to the ambient pressure that is defined as being zero. Thus

$$\bar{p}_{z=\pm L/2} = 0. \quad (9)$$

At the point of film rupture, the pressure boundary conditions are

$$\bar{p} = \frac{\partial \bar{p}}{\partial \theta} = 0 \text{ at } \theta = \theta^*. \quad (10)$$

At the ends of bearing, it is reasonable to assume that no heat will be transferred to the surrounding in the axial direction at the ends of the bearing. That is, the oil temperature having come out to the surrounding is assumed the same as of that at the end of the bearing, so

$$q_{z=\pm L/2} = 0. \quad (11)$$

For oil mixing condition, at the groove, the oil temperature is assumed as the mixing temperature between the re-circulating oil and inlet oil as shown on Fig. 1. The detailed expression is

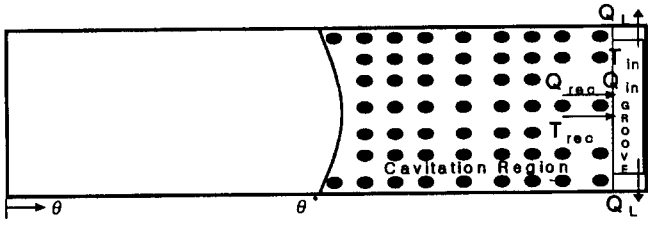

Fig. 1. Diagram of lubricant flow.

defined as

$$T_{mix} = \frac{(Q_{in} - Q_L)T_{in} + L_c Q_{rec} T_{rec}}{(Q_{in} - Q_L) + L_c Q_{rec}}. \quad (12)$$

where is the inlet oil flow rate, the re-circulating flow rate and the side oil flow rate going through groove land. is the angle of the beginning of the cavitation region. is contraction ratio [17] of oil film that defined as

$$L_c(\theta) = \frac{\int_{-L/2}^{L/2}\int_0^{h(\theta^*, z)} u(\theta^*, z)dydz}{\int_{-L/2}^{L/2}\int_0^{h(\theta, z)} u(\theta, z)dydz}. \quad (13)$$

This ratio is the effective wetted width of the bush in the cavitating region. Then the heat transfer coefficient to the bush, adjusted for the reduction of wetting area in the cavitating region by the contraction ratio, becomes $H_b = L_c H_{bo} + (1 - L_c)H_{bg}$.

Calculation of Parameters

The non-dimensional load parameter components $\overline{W_c}$ and $\overline{W_p}$, parallel and normal to the line of centers respectively, are given by:

$$\overline{W_c} = \frac{W_c}{LD}\left(\frac{c}{R}\right)^2\left(\frac{L}{D}\right)/\mu_o N = -\frac{1}{4}\int_0^{2\pi}\int_{-L/D}^{L/D} \bar{p}cos\theta d\bar{z}d\theta \quad (14a)$$

and

$$\overline{W_p} = \frac{W_p}{LD}\left(\frac{c}{R}\right)^2\left(\frac{L}{D}\right)/\mu_o N = \frac{1}{4}\int_0^{2\pi}\int_{-L/D}^{L/D} \bar{p}sin\theta d\bar{z}d\theta. \quad (14b)$$

Note that the total load parameter, $\overline{W}$, will be

$$\overline{W} = \sqrt{(\overline{W^2}_c + \overline{W^2}_p)}. \quad (14c)$$

For turbulent flow, the non-dimensional form of total friction force [18] can be expressed as follows

$$\overline{F_t} = \frac{F_t}{LD}\left(\frac{c}{R}\right)\left(\frac{L}{D}\right)/\mu_o N = \frac{1}{4}\int_0^{2\pi}\int_{-\frac{L}{d}}^{\frac{L}{D}}\left(G_x\frac{H}{2}\frac{\partial \bar{p}}{\partial \theta} + \bar{\tau}_c\mu\frac{2\pi}{H}\right)d\bar{z}d\theta \quad (15)$$

The frictional torque is equal to friction force multiplied by the radius of a bearing and the frictional power loss is friction force multiplied by the velocity of the bearing shaft.

The non-dimensional form of side leakage for turbulent

lubrication [18] is :

$$\bar{Q}_{zt} = \frac{Q_{zt}}{NcR^2} = -\int_0^{2\pi} G_z \frac{H^3}{\bar{\mu}} \frac{\partial \bar{p}}{\partial \bar{z}}\bigg|_{\bar{z} = \pm L/D} d\theta . \quad (16)$$

Computation

The turbulent Reynolds and the energy equations with turbulent similarity parameters have been solved by finite difference method using successive-over-relaxation iteration. The central finite difference technique is applied to the non-dimensional Reynolds equation. The backward difference scheme in the circumferential direction, and backward and forward difference schemes in the axial direction are used to the non-dimensional energy equation. The grid used comprises 43×15 nodes. The relaxation parameter used is 1.73 for Reynolds equation. However, for the energy equation, the parameter is 1.01.

To speed up the solution procedure, the Reynolds equation is solved by firstly assuming isothermal conditions to obtain an initial flow field for other thermal conditions. With the initial values, the energy equation is solved together with Reynolds equation. For the cases with very low oil input temperatures, convergence improves if the viscosity is constrained to change gradually from the isothermal distribution to the final one. With the pressure and temperature distributions thus specified, the load, friction and side leakage parameters can then be computed from equation (14c), (15) and (16).

Results and Discussions

In this section, the effect of the thermal boundary conditions on turbulent film bearings (isothermal, adiabatic and convective) is examined. Previous work [12] indicated that adiabatic conditions were a good approximation for thick turbulent films. It would be of interest to investigate the relation of these results with equivalent results with different thermal conditions. The bearing geometry parameters and the lubricant properties used, are summarized in Table 1. A bearing with one axial groove will be examined. As the results of the calculation, the contraction ratio varies from 0.98 (at the starting position of cavitation) to 0.26 (at the ending position of cavitation) for aligned bearings and from 0.99 to 0.31 for misaligned bearings. The basic algorithm of a numerical model used for this study had been verified by Chun [19].

Table 1. Journal bearing operating conditions.

Bearing Diameter	D = 73.6 mm
L/D Ratio	0.5
c/R Ratio	0.0039837
Eccentricity Ratio	ε = 0.65
Rotational Speed	N = 40,000 rpm
Lubricant Viscosity at 40°C	μ_o = 0.0236 Pa · s
Temperature-viscosity Coefficient	α = 0.028 K^{-1}
Lubricant Density at 40°C	ρ = 860Kg/m^3
Lubricant Specific Heat	C_p = 2000 J/kg°C
Heat Transfer Coefficient of Lubricant to Bush	H_{bo} =7700 W/m^2°C
Heat Transfer Coefficient of Gas(Air) to Bush	H_{bo} =2400 W/m^2°C
Heat Transfer Coefficient of Lubricant to Shaft	H_s =7700 W/m^2°C
Bush and Shaft Temperature	$T_{b,s}$ = 45°C
Inlet Lubricant Temperature	T_{in} = 40°C
Inlet Lubricant Pressure	P_{in} = 0.7 × 10^5 Pa
Axial Groove Width	17.1°(2 grid intervals)

Table 2 shows the results for the non-dimensional load, friction and axial leakage, as well as the maximum film pressure and temperature for the aligned bearing with an axial groove operating at the conditions specified in Table 1. For all configurations, the inclusion of realistic boundary conditions on temperature resulted in substantial reduction of the load capacity of the bearing. The reduction is approximately 80 percent. The changes in friction follow the same trend but are reaching 66 percent. These changes are easily interpreted by studying the accompanying maximum temperatures. As the temperature rises and correspondingly the viscosity falls, the load and friction decreases noticeably and the axial leakage increases slightly.

From Table 2, it is observed that the isothermal results, excepting the axial leakage, are around twice the results under the other two conditions considering no flow mixing and around 3 to 8 times the results under the other two conditions considering flow mixing. It is interested that the influence of

Table 2. Non-dimensional load, friction force and axial leakage, as well as the maximum oil film pressure (in MPa) and temperature (in °C) for an aligned bearing with an axial groove.

Boundary Conditions	Case No.1 (Isothermal)	Case No.2 (Adiabatic, No Mixing)	Case No.3 (Convective, No Mixing)	Case No.4 (Adiabatic, Mixing)	Case No.5 (Convective, Mixing
Load	2.387	1.230	1.248	0.324	0.469
Friction force	16.222	9.681	9.809	4.565	5.495
Axial Leakage	0.320	0.353	0.350	0.368	0.359
Max. Oil Pressure	13.508	6.556	6.658	1.679	2.479
Max Oil Temperature	40.00	112.82	106.97	187.26	141.08

Table 3. Non-dimensional load, friction force and axial leakage, as well as maximum oil film pressure (in MPa) and temperature (in °C) for an aligned bearing operating at the conditions specified in Table 1 with bush and shaft wall temperatures as indicated.

Boundary Conditions	Case No.1 (Isothermal)	Case No.2 (Adiabatic, No Mixing)	Case No.3 (Convective, No Mixing)	Case No.4 (Adiabatic, Mixing)	Case No.5 (Convective, Mixing)
a. Wall Temperature = 20°C					
Load	2.384	1.230	1.326	0.324	0.512
Friction force	16.222	9.681	10.366	4.565	5.742
Axial Leakage	0.320	0.353	0.349	0.368	0.357
Max. Oil Pressure	13.508	6.556	6.883	1.679	2.721
Max. Oil Temperature	40.00	112.82	103.63	187.26	133.49
b. Wall Temperature = 45°C (see Table 2)					
c. Wall Temperature = 80°C					
Load	2.384	1.230	1.232	0.324	0.416
Friction force	16.222	9.681	9.707	4.565	5.177
Axial Leakage	0.320	0.353	0.352	0.368	0.362
Max. Oil Pressure	13.508	6.556	6.354	1.679	2.182
Max. Oil Temperature	40.00	112.82	111.70	187.26	152.88

Table 4. Non-dimensional load, friction force and axial leakage, as well as maximum oil film pressure (in MPa) and temperature (in °C) for an aligned bearing operating at the conditions specified in Table 1 with inlet oil temperature as noted.

Boundary Conditions	Case No.1 (Isothermal)	Case No.2 (Adiabatic, No Mixing)	Case No.3 (Convective, No Mixing)	Case No.4 (Adiabatic, Mixing)	Case No.5 (Convective, Mixing)
a. Inlet Oil Temperature = 20°C					
Load	3.991	1.664	1.656	0.350	0.502
Friction force	25.852	12.393	12.412	4.749	5.681
Axial Leakage	0.314	0.358	0.356	0.366	0.357
Max. Oil Pressure	22.718	8.410	8.379	1.823	2.654
Max. Oil Temperature	20.00	105.86	101.36	173.52	134.92
b. Inlet Oil Temperature = 40°C (see Table 2)					
c. Inlet Oil Temperature = 80°C					
Load	0.986	0.723	0.759	0.289	0.415
Friction force	8.801	7.081	7.298	4.299	5.184
Axial Leakage	0.338	0.351	0.349	0.373	0.363
Max. Oil Pressure	5.497	3.807	4.023	1.494	2.188
Max. Oil Temperature	80.00	133.47	122.84	218.25	155.14

the boundary conditions at the wall is the relatively small compared with the mixing details at the inlet port. Under no mixing condition, the difference of parameters between convective and adiabatic conditions is very small as below 2 percent. On the contrary, under mixing condition, the difference of parameters between convective and adiabatic conditions shows a remarkable contrast as around 30 percent. The differences of parameters between no mixing and mixing conditions show up to 70 percent for adiabatic condition and 60 percent for convective condition. Thus, the main differences are between conditions No. 2 and No. 4 (or between No. 3 and No. 5) that are resulted in the details of the mixing process at the groove. The flow mixing become important in determining the temperature of the oil in the downstream around oil inlet port. In case No. 2 and No. 3, it is lower since it is essentially the oil inlet temperature (40°C). While for case No. 4 and No. 5, it is higher by 50 to 70°C with correspondingly lower viscosity.

To explore the effect of the thermal distribution further, the influence of the wall temperature has also been examined. In Table 3, load, friction and axial leakage parameters are presented for the bush and shaft wall temperature of 20°C and 80°C in addition to the previous ones of 45°C. Despite the different temperatures imposed, the trend remains the same. The higher temperatures result in lower load, lower friction and slightly higher leakage in both cases of the 80°C and the 20°C

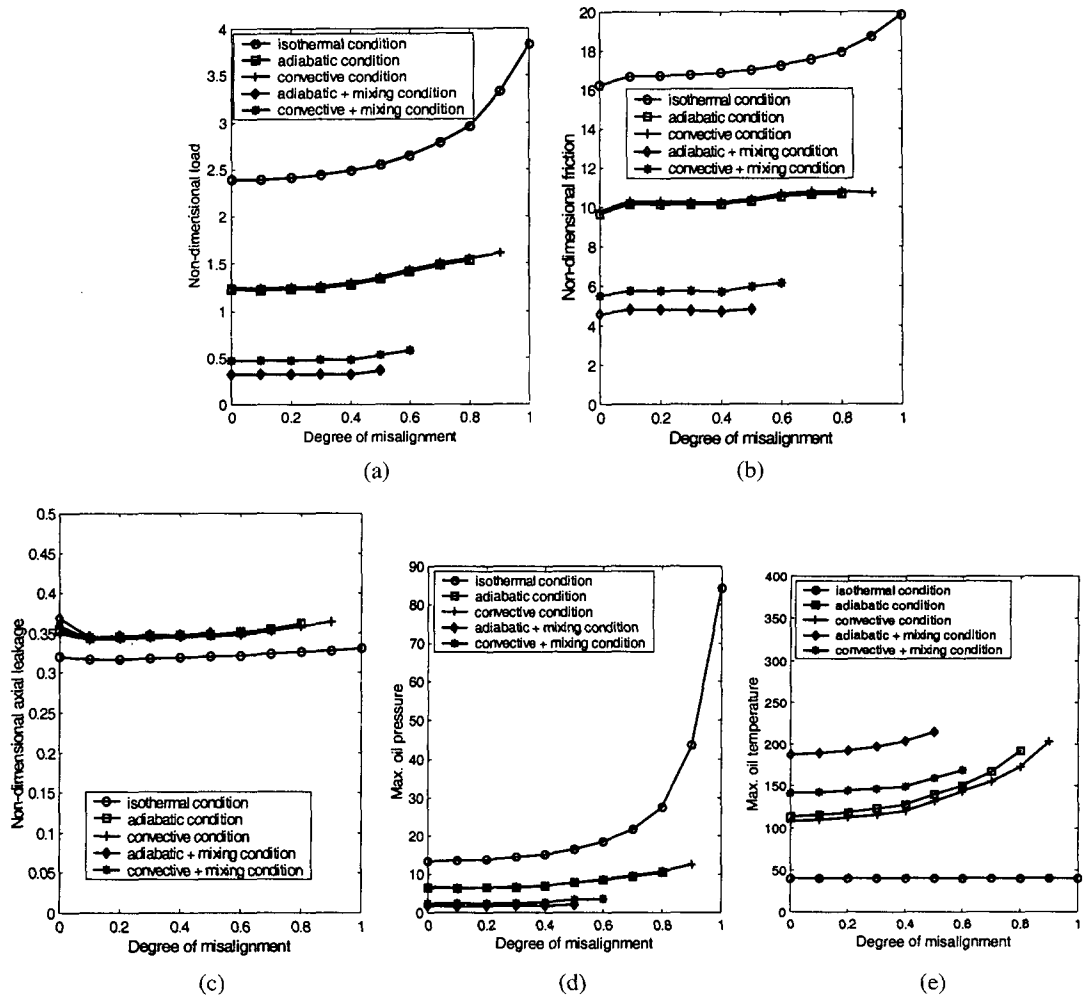

Fig. 2 Non-dimensional load, friction and axial leakage, as well as the maximum oil film pressure (in MPa) and temperature (in °C) vs. degree of misalignment at various thermal boundary conditions. (a) Non-dimensional load, (b) Non-dimensional friction force, (c) Non-dimensional axial leakage, (d) Maximum oil film pressure, (e) Maximum oil film temperature.

wall. Despite the large increase and decrease of the wall temperature, the changes in load remain less than 9 percent compared to 70 percent caused by the difference in mixing at the inlet. The changes in friction remain less than 6 percent compared to 50 percent caused by the difference in mixing at the inlet. Thus, the big changes of wall temperature just show small changes in the load and friction. The high temperature field is then seen to be the dominant factor in determining the viscosity and indirectly the load and friction.

This effect becomes more pronounced when the inlet temperature of the oil is varied. In Table 4, the values for the load, friction and leakage for three different oil inlet temperatures are presented. The viscosity-temperature coefficients are 0.029 for 20°C and 0.025 for 80°C. The viscosities at each inlet temperature are 0.0420 for 20°C and 0.0078 for 80°C. To obtain the non-dimensional load and friction with the reference viscosity at 40°C, the 20°C calculated values were multiplied by 1.7797 and the 80°C ones by 0.3305. The influences of mixing on the load and friction are about 1.5 times that of the boundary conditions at the walls under the high oil inlet temperature but 2.5 times under low oil inlet temperature. The difference of the load between results with constant viscosity and variable viscosity varies between 60 percent at high oil inlet temperature to 90 percent at low temperature under the condition No. 5. The friction also changes by 40 percent at high values of the inlet temperature and by 80 percent at the low inlet temperature under the condition No. 5. This is because the heat generated by friction in the oil film of the bearing is not as significant as its internal energy when the oil is at higher temperatures. The changes between conditions No. 2 and No. 3 (and also between No. 4 and No. 5), i.e. between adiabatic and convective conditions at the walls, are again much smaller than the ones between No. 2 and No. 4 (and also between No. 3 and No. 5), which are due to the details of mixing. Of interest is also the variation of the leakage rate. The effects of the oil inlet temperature on the side leakage seem to be very small under high shaft speed. The reason is that relatively small values in pressure gradient in axial direction are expected.

In most operational situations with variable conditions, the probability is great that journal bearings will be subjected to uneven loads resulting in misalignment. Thus to complete out

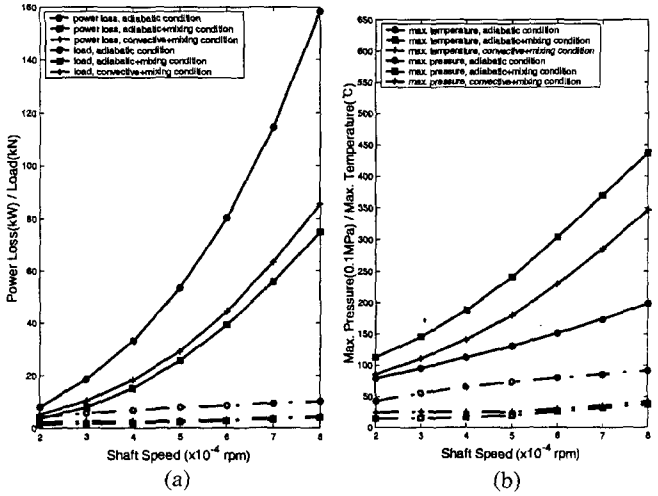

Fig. 3. (a) Load capacity and power loss vs. shaft speed for an aligned bearing at various thermal conditions. (b) Maximum pressure and temperature vs. shaft speed for an aligned bearing at various thermal conditions

this study, a set of computations was carried for various degrees of misalignment. The misalignment was considered to be only in the plane of the eccentricity vector. Thus misalignment degree, D_m, refers to the percentage reduction of the minimum film thickness at the bearing ends. Consequently, $D_m = 1.0$ implies that the shaft is touching at top and bottom at the ends of the bearing. The results of the computations under conditions Nos. 1 to 5 are shown in Fig. 2. The results could only be obtained up to more or less 200°C of maximum oil temperature due to computation overflow or underflow. As the degree of misalignment increases, the non-dimensional parameters increase slightly regardless of adiabatic and convective conditions. Thus, misalignment effects on the load and friction are reduced substantially when the temperature variation is included. Under no mixing condition, the differences in the values of parameters between adiabatic and convective condition are very small all the way to higher degrees of misalignment. However, under mixing condition, excepting the axial leakage, the differences in the values of parameters between convective and adiabatic conditions remain around 30 percent through all degrees of misalignment.

In Fig. 3a, the power loss and the load capacity vs. the shaft speed are plotted for various thermal conditions. The faster the shaft rotates, the higher the load and power loss are. However, the change of load is relatively small compared to the power loss. This is surprising since in Fig. 3b the maximum pressure is found to vary weakly with the shaft speed whereas the temperature changes dramatically. One would have expected a similarly weak increase in power loss since the high temperature would result in substantially lower viscosity despite the strong dependence of the friction on speed. By the mixing between the re-circulating flow and the inlet flow, the maximum oil temperature increases. Then, the load, the power loss and the maximum pressure decrease through all ranges of shaft speed. Implying realistic mixing condition, the results in the power loss and the temperature under adiabatic boundary condition show clear differences as comparing with those under convective condition.

Conclusions

In studying the behavior of a high-speed journal bearing generating turbulent motion, it is found that the inclusion of more realistic convection boundary condition at the walls under no mixing condition does not result in noticeable differences from the usual adiabatic wall results. However, under mixing condition, the convective boundary condition cannot be substituted by the adiabatic boundary condition for the design purpose of journal bearing. The mixing process of the re-circulating oil with the incoming supply oil at the groove plays an important role in determining the temperature distribution. The wall temperature has been found not to affect the load and friction substantially. The lower the temperature of the inlet oil, the larger the temperature gradient in the film and the greater the need to include the energy equation in the calculations for acceptable accuracy. Misalignment effects on load and friction are reduced substantially when temperature variation is included. The most dominant factor for frictional loss for turbulent conditions is the high shaft speed.

Nomenclature

c = radial clearance between journal and its bearing (m)
C_p = specific heat of lubricant(kJ/kg°C)
D = bearing diameter (m)
D_m = degree of misalignment (the percentage reduction of minimum film thickness at the bearing ends)
e = eccentricity(the offset distance between journal and bearing centers)
F = friction force
$\bar{F}$ = non-dimensional friction force $((F/LD)\ (c/R)/(\mu_o N)(L/D))$
$G_{x,z}$ = Similarity parameters
h = oil film thickness (m)
H = non-dimensional film thickness (h/c)
H_b = convective heat transfer coefficient to bush (W/m^2°C)
H_{bg} = convective heat transfer coefficient of gas(air) to bush (W/m^2°C)
H_{bo} = convective heat transfer coefficient of oil to bush (W/m^2°C)
H_s = convective heat transfer coefficient to shaft (W/m^2°C)
L = bearing length (m)
L_c = contraction ratio of oil film
N = rotational speed (rpm)
$\bar{p}$ = mean pressure for turbulent flow(Pa)
$\bar{\bar{p}}$ = non-dimensional mean pressure $(\bar{p}(c/R)^2/\mu_o N)$
$\bar{\bar{p}}$ = non-dimensional effective pressure $(H^{3/2}\bar{P}/\bar{\mu}^{1/2})$
P_{in} = inlet pressure (Pa)
$q_{bT,sT}$ = turbulent heat transfer to the bush and shaft (W)
Q_{in} = inlet oil flow rate (m^3/s)
Q_L = side oil flow rate through groove land (m^3/s)

Q_{rec} = re-circulating oil flow rate (m^3/s)
Q_{zl} = lubricant side leakage (m^3/s)
$\bar{Q}_{zl}$ = non-dimensional lubricant side leakage (Q_{zl}/NcR^2)
R = journal bearing radius (m)

Re = Reynolds number ($\frac{\rho Uh}{\mu}$)

$\bar{T}$ = mean temperature for turbulent flow(°C)
$\bar{\bar{T}}$ = non-dimensional mean temperature

$$\left(\frac{\rho C_o (c/R)^2}{2\pi\mu_o N}(\bar{T} - T_{in})\right)$$

T_{in} = inlet temperature (°C)
T_b = temperature of the bush (°C)
T_{mix} = mixing temperature at groove (°C)
T_{rec} = re-circulating temperature (°C)
T_s = temperature of the shaft (°C)
u = velocity of lubricant (m/s)
U = speed of journal (m/s)
W = applied load
$\bar{W}$ = non-dimensional load parameter

$$\left(\frac{W}{LD}\left(\frac{c}{R}\right)^2\left(\frac{L}{D}\right)/(\mu_o N)\right)$$

x,z = coordinates of circumferential and axial directions, respectively
$\theta, \bar{z}$ = non-dimensional coordinates ($\theta = x/R$, $\bar{z} = z/R$)
ϑ^* = position of film rupture
α = viscosity-temperature coefficient(1/K)
β = tilt angle of a shaft
ε = eccentricity ratio = e/c
η = misalignment ratio ()
μ = lubricant viscosity (Pa.s)
μ_o = inlet lubricant viscosity (Pa.s)
$\bar{\mu}$ = (μ/μ_o)
ρ = lubricant density (kg/m^3)
ϕ = misalignment directional angle, i.e., the angle between the plane of the misalignment and the axial plane containing the load vector
φ = attitude angle, i.e., angle between the line of centers and the axial plane containing the load vector
τ_c = Couette shear stress

$\bar{\tau}_c$ = Similarity parameter ($\tau_c/\frac{\mu U}{h}$)

References

1. Wilcock, D. F., Turbulence in High Speed Journal Bearing, Trans. of the ASME, Vol. 72, pp. 825-834, 1950.
2. Constantinescu, V. N, Theory of Turbulent Lubrication, Proc. Int. Symp. on Lubrication and Wear, University of Houston, pp. 153-213., 1965.
3. Ng, C. W. and Pan, C. H. T., A Linearized Turbulent Lubrication Theory, Trans. of the ASME, J. of Basic Engineering, Vol. 87, pp. 675-688, 1965.
4. Taylor, C. M., Turbulent Lubrication Theory Applied to fluid Film Bearing Design, Proc. Inst. Mech. Engrs., Vol. 184, Part 3L, pp. 40-47, 1969-1970.
5. Constantinescu, V. N., Basic Relationships in Turbulent Lubrication and Their Extension to Include Thermal Effects, Trans. of the ASME, J. of Lubrication Technology, Vol. 95, pp. 147-154, 1973.
6. Safar, Z. and Szeri, A. Z., Thermohydrodynamic Lubrication in Laminar and Turbulent Regimes, Trans. of the ASME, J. of Lubrication Technology, Vol. 96, pp. 48-57, 1974.
7. Szeri, A. Z., Tribology: Friction, Lubrication and Wear, Chapter 5, Turbulence, Inertia, and Thermal Effects in Fluid Film Bearings, Hemisphere Publishing Corp., pp. 229-294, 1980.
8. Hashimoto, H., Thermohydrodynamic Lubrication Theory for Turbulent Journal Bearings with Surface Roughness (1st Report, Modified Energy Equation and Adiabatic Approximate Solution). Transactions of the Japan Society of Mechanical Engineers, Part C. 57, No. 539, pp. 2414-2421, 1991.
9. Suganami, T. and Szeri, A. Z., A Thermohydrodynamic Analysis of Journal Bearings, Trans. of the ASME, J. of Lubrication Technology, Vol. 101, pp. 21-27, 1979.
10. Suganami, T. and Szeri, A. Z., A Parametric Study of Journal Bearing Performance: The 80 deg Partial Arc Bearing, Trans. of the ASME, J. of Lubrication Technology, Vol. 101, pp. 486-491, 1979.
11. Medwell, J. O. and Bunce, J. K., The Influence of Bearing Inlet Conditions on Bush Temperature Fields, Proceedings of the 6th Leeds-Lyon Symposium on Tribology, Thermal Effects in Tribology, Published by Mech. Eng. Publ. Ltd., pp. 56-64, 1980.
12. Medwell, J. O. and Gethin, D. T., Synthesis of Thermal Effects in Misaligned Hydrodynamic Journal Bearings, International Journal for Numerical Methods in Fluids, Vol. 6, pp. 445-458, 1986.
13. Safar, Z. and Raid, M. S. M., Prediction of the Coefficient of Friction of a Misaligned Turbulent Flow Journal Bearing, Tribology International, Vol. 21, pp. 15-19, 1988.
14. Cebeci, T. and Smith, A. M. O., Analysis of Turbulent Boundary Layers, Academic Press Inc., Chapter 1-3, 1974.
15. Gazley, C. Jr., Heat-Transfer Characteristics of the Rotational Axial Flow Between Concentric Cylinders, Trans. of the ASME, Vol. 80, pp. 79-90, 1958.
16. Smalley, A. J. and McCallion, H., The effect of Journal Misalignment on Performance of a Journal Bearing under Steady Running Conditions, Proc. Inst. Mech. Engrs., Vol. 181, Part 3B, pp. 45-54, 1966-1967.
17. Boncompain, R., Fillon, M. and Frene, J., Analysis of Thermal Effects in Hydrodynamic Bearings, Trans. of the ASME, Vol. 108, pp. 219-224, 1986.
18. Snech, H. J. and Vohr, J. H., Handbook of Lubrication (Theory and Practice of Tribology), Volume II, Theory and Design, Hydrodynamic Lubrication, CRC Press, Inc., pp. 73-79, 1984.
19. Chun, S. M. And Jang S., A Study on Turbulent Lubrication of Journal Bearings Considering Proceedings of 7th Australasian Heat an Mass Transfer Conference, James Cook University in Townsville, Queensland, Australia, July 3rd-6th, pp. 97-104, 2000.